Dual-Band Loop-Loaded Printed Dipole Antenna with a Wideband Microstrip Balun Structure

Mustafa H. B. Ucar, Adnan Sondas, and Yunus E. Erdemli

Electronics & Computer Education Department
Kocaeli University, Umuttepe Campus, 41380 Kocaeli, Turkey
mhbucar@kocaeli.edu.tr, asondas@kocaeli.edu.tr, yunusee@koceli.edu.tr

Abstract ─ A novel loop-loaded printed dipole (LLPD) with a wideband balun structure is presented for aiming a dual-band antenna operation at 3.0/5.5 GHz bands. The proposed balun structure alone demonstrates VSWR<1.5 performance over a 3:1 bandwidth. As the loop elements placed on the antenna aperture provides dual-band operation with at least 15% impedance bandwidths, the wideband balun/feed allows for matched and balanced excitation for the dipole over the bands of interest. An equivalent circuit modeling of the LLPD antenna is presented along with the corresponding simulations and measurements.

Index Terms ─ Balun/feed, dual-band operation, equivalent circuit model, loop elements, printed dipole.

I. INTRODUCTION

Compact multi-function antennas play a major role in today's communication systems where size, weight, power consumption and cost are the key issues in designing integrated transceiver circuitry. In this context, printed antennas were previously considered to achieve multi-band or wideband applications [1−16]. Printed dipole elements, in particular, are preferred in such applications due to their low-profile and easy fabrication. The dipoles, however, cannot perform in the way as predicted when they are excited directly by a coaxial feed. This is due to inherit unbalanced current excitation by the coax. To overcome this undesired phenomenon, a balun (balanced-to-unbalanced) structure is required in the coax-fed dipole applications in order to match the unbalanced coaxial transmission line to the balanced two-wire line, i.e. the dipole in this case.

In this study, a novel loop-loaded printed dipole (LLPD) with a wideband balun structure is introduced for a dual-band antenna operation at 3.0/5.5 GHz bands, which are designated for a specific radar application. Recently, parasitic or loading elements have been considered to obtain dual-band dipole operation [9, 10]. A dual-band printed dipole antenna with a multi-arm parasitic element is introduced in [9] for WiMAX applications covering the bands 2.5–3.8 GHz and 5.15–5.85 GHz. In [10], an antipodal printed dipole loaded with circular split-ring resonator (SRR) elements has been introduced for a dual-frequency operation. In that study, eight SRR elements consisting of two concentric split-rings each are placed along the length of the dipole to achieve a dual-band operation at 1.2 GHz and 2 GHz bands. Also in [11], the authors have recently introduced a twisted dipole antenna with switchable loadings to achieve tunable antenna operation for 3.0 GHz and 5.5 GHz bands.

In this research, we propose a novel printed dipole antenna loaded with two rectangular loop elements (without splits) asymmetrically placed along the dipole length to achieve the dual-band operation around the center frequencies of 3 GHz and 5.5 GHz. As compared to its counterparts [9, 10], the proposed LLPD configuration is rather simple in structure, thus offers more flexibility in designing for different operational frequencies while maintaining the desired antenna performance.

It is worth mentioning that the proposed antenna is low-cost, low-loss, low-profile, and is also arrayable [17]. We note that the full-wave

Submitted On: Jan. 26, 2012
Accepted On: April 25, 2012

1054-4887 © 2012 ACES

analysis of the antenna design has been carried out using CST Microwave Studio, which utilizes the time-domain finite-integration method. In this article, we present the corresponding simulation and measurement results to demonstrate the performance of the proposed LLPD design. In addition, several parametric studies are presented to show the design flexibility of the proposed configuration. A simplistic equivalent circuit modeling of the LLPD is also presented.

II. ANTENNA AND BALUN/FEED DESIGN

The proposed LLPD/balun configuration is depicted in Fig. 1 along with the corresponding physical parameters. As shown, the antenna aperture consists of a printed dipole and a doublet of concentric loop elements asymmetrically located (at a distance of 0.3 mm) on each side of the dipole feed-gap, which is 0.89 mm. All these elements are supported by a thin substrate with t=0.79 mm and ε_r=2.2 (Arlon DiClad 880). While the dipole by itself resonates around 3 GHz, the inclusion of the loop elements allows for an additional operational frequency band around 5.5 GHz. The loop elements provide not only inherent inductive loading, but also capacitive loading to the dipole, thus achieving 50Ω matched dual-band operation. In particular, the capacitive effect occurs due to proximity of the loop elements to the dipole as well as interaction between the concentric loop elements. We remark that the critical parameters to achieve the desired dual-band performance are the loop dimensions, the effects of which on the antenna operation will be discussed in Section III.

When the dipole was excited directly by a coax-feed, the realized antenna could not perform in the way the simulations predicted [18]. This "expected" phenomenon is mainly due to the unbalanced behavior of the coax. Hence, a new balun structure having compatible conjunction with the dipole has been designed. As shown in Fig. 1, the LLPD is excited by a balun-feed structure placed vertically between the aperture and the ground plane (GP) where the aperture-GP distance is set to h=17 mm. This novel balun structure has a tapered microstripline with metallic extensions, and is supported by a similar substrate (t=0.79 mm, ε_r=2.2) placed on a triangular-shaped GP as depicted in detail in Fig. 2. The triangular shape [19] is chosen to accommodate the balun structure underneath the dipole gap appropriately. More importantly, the shape, position, and size of those extensions placed along the microstripline are determined to be the critical parameters of the balun design to achieve wideband VSWR performance. We note that for optimum performance the design parameters of the LLPD were re-optimized in integration with the balun-feed.

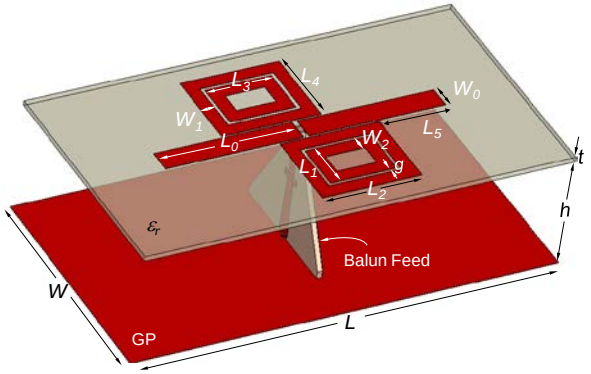

Fig. 1. The proposed LLPD/balun configuration: W=36, L=66, W_0=3.5, L_0=21.2, L_1=7.4, L_2=15.7, L_3=10.5, L_4=12.4, L_5=10.3, W_1=2.1, W_2=2, g= 0.5, t= 0.79, h= 17 (all in mm), ε_r=2.2.

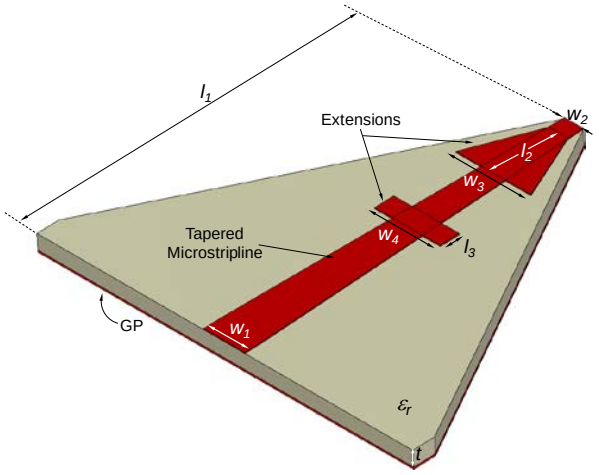

Fig. 2. The proposed balun configuration: l_1=18.275, l_2=3.4, l_3=1, w_1=2.2, w_2=1, w_3=4, w_4=3.5, t=0.79 (all in mm), ε_r=2.2.

III. RESULTS AND DISCUSSIONS

The simulated and measured VSWR characteristics of the back-to-back balun structure are displayed in Fig. 3. As shown, the realized

balun design with the extensions provides VSWR<1.5 over 2–6 GHz band, i.e. a 3:1 bandwidth. Also displayed in Fig. 3 are the results for the balun design without extensions, yielding relatively worse VSWR levels (around 1.5–2) for frequencies below 4.5 GHz. That is, the metallic extensions placed along the microstripline play a key role for better matching in lower frequencies. Also note that the measured data show ripple characteristics tracking the rather smooth simulated profile, mainly due to the standing-wave phenomenon observed in the measurements.

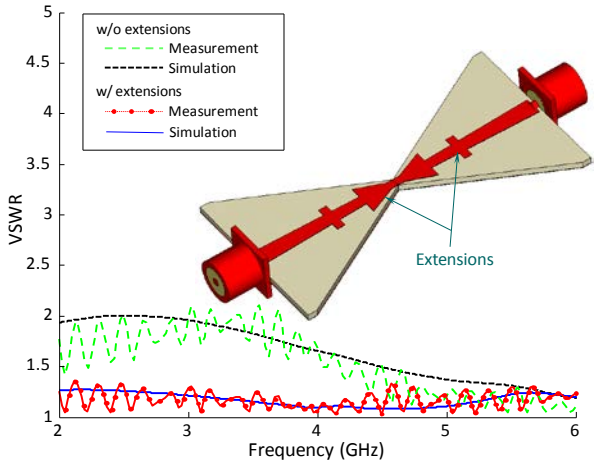

Fig. 3. The simulated and measured VSWR results for the balun designs.

Having discussed the balun design by itself, we now consider the performance of the LLPD antenna integrated with the balun-feed structure. The photograph of the fabricated LLPD/balun antenna is depicted in Fig. 4. In Fig. 5, we display the simulated and measured input reflection coefficient (S_{11}) characteristics of the LLPD design along with the corresponding bandwidth performances listed in Table 1. As seen, the agreement between the results is quite good except that a little amount of bandwidth reduction (~1.5%) is observed for the fabricated antenna. The discrepancies are probably due to material and fabrication tolerances. Of importance is that the realized antenna offers a dual-band operation with at least 15% S_{11} bandwidth at each band of interest, i.e. 3 GHz and 5.5 GHz where $|S_{11}|<-10$ dB criterion along with 50Ω system is considered. We note that the VSWR and return loss measurements were carried out using Rohde & Schwarz ZVB8 Vector Network Analyzer.

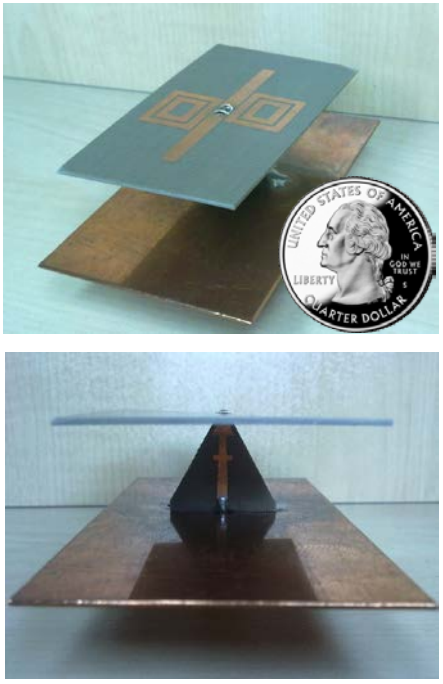

Fig. 4. The perspective views of the fabricated LLPD antenna.

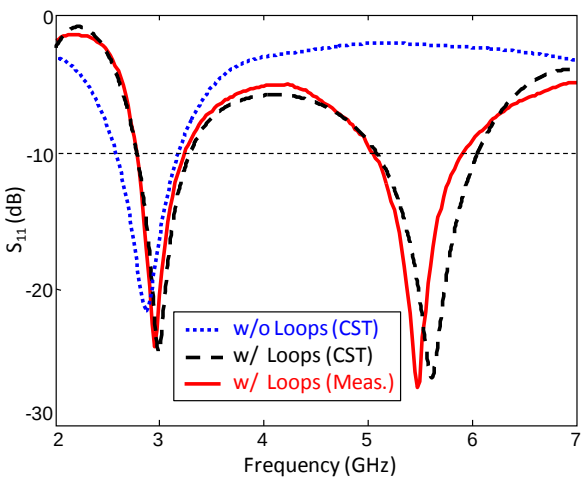

Fig. 5. The input reflection coefficient characteristics of the LLPD/balun design: the CST simulations for the cases with and without loop elements, and the measured results for the fabricated antenna with the loops are shown.

Also in Fig. 5, the simulated S_{11} performance of the dipole in absence of the loop elements is shown besides that of the LLPD design, where the loops play a key role in the occurrence of the upper frequency-band. In fact, the inclusion of the loops causes an additional resonance as well as an improvement in impedance matching in the upper

band as shown in Fig. 6, where the input impedance at the balun-coax end is displayed for the cases without and with the loops. As seen, for the former case, there are two resonances around 2.7 GHz and 4.8 GHz where the real part of impedance levels reaches 400 Ohms. On the other hand, for the latter case, an additional resonance occurs around 5.5 GHz, while the previous 4.8 GHz band shifts downwards to 4.2 GHz due to the loading effect of the loops. In addition, there is a slight upward shift observed in the lower band as can be seen from Figs. 5 and 6. More importantly, the impedances are dramatically reduced to 50 Ω levels owing to the inclusion of the loops, thus a desired matching is achieved around 5.5 GHz band.

Table 1: Bandwidth (BW) comparison of the simulated and fabricated antennas

Band	Simulation (CST)	Measurement
3.0 GHz	2.78–3.29 GHz BW~16.8%	2.78–3.24 GHz BW~15.3%
5.5 GHz	5.07–6.06 GHz BW~17.8%	5.03–5.92 GHz BW~16.3%

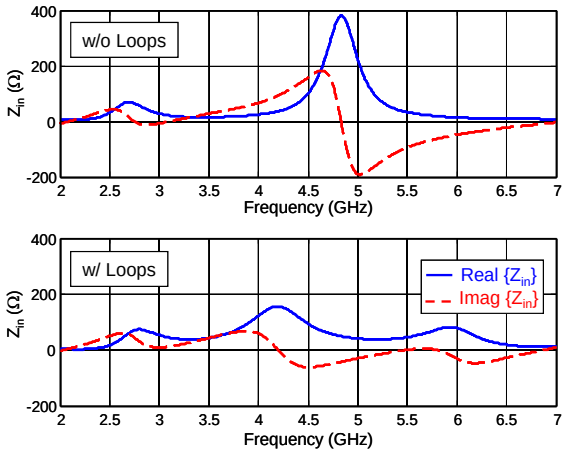

Fig. 6. The simulated input impedances (Z_{in}) for the cases without (top) and with (bottom) the loops.

In Fig. 7, we also display the computed surface current distributions over the antenna aperture for both frequency bands. As seen, the current distribution at 3 GHz is mainly concentrated along the dipole, while the distribution at 5.5 GHz is predominantly occurs around the loops as well as between the dipole and the loops. These results also confirm that the lower frequency band is mainly due to the dipole resonance, but the higher band occurs owing to presence of the loop elements.

In addition, we carried out radiation pattern measurements for the LLPD/balun configuration in an anechoic chamber using ETS-Lindgren 3117 DRG horn antenna (1–18 GHz). The computed and measured radiation patterns at 3 GHz and 5.5 GHz are displayed in Fig. 8 where a reasonably well agreement is observed. As shown, the antenna offers a broadside radiation pattern with a directive gain of about 7.5 dBi at the respective frequencies, where the front-to-back ratios are predicted as being higher than 13 dB. In addition, the computed radiation efficiency of the LLPD antenna is better than 95% at the related frequencies.

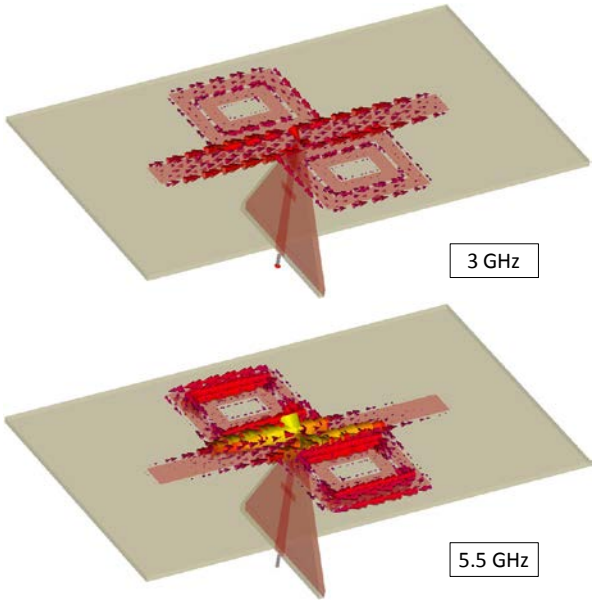

Fig. 7. The surface current distributions over the antenna aperture at 3 GHz (top) and 5.5 GHz (bottom).

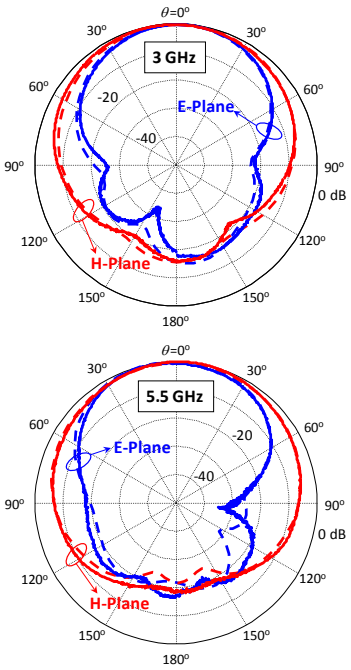

Fig. 8. The computed (dashed) and measured (solid) radiation patterns of the LLPD/balun design at 3 GHz (top) and 5.5 GHz (bottom).

Although the presented design is projected for a specific frequency operation, one can obtain a similar dual-band performance at different operational frequencies by varying some parameters of the antenna structure. In designing, we have carried out several parametric studies to achieve the optimum antenna performance. Here, we present those studies performed for the three critical design parameters, namely, the dipole length ($2L_0$) and the loop dimensions (L_2 and L_4). As can be seen from Fig. 9, the dipole length mainly determines the lower-band, while the loop dimensions play a major role in occurrence of the higher-band. Of importance is that when the dipole length is fixed, by varying the loop size one can shift the higher-band upwards or downwards with an insignificant effect on the lower-band (Fig. 9 (b) and (c)). Similarly, by varying the dipole length with the loop size fixed, one can shift the lower-band accordingly (Fig. 9 (a)). In brief, those studies demonstrate the flexibility of the proposed LLPD configuration; thus, provide some guidelines in designing for a different set of dual frequencies.

In addition, other loop parameters have also been examined during the design optimization process. The presence of inner loops is shown to have a critical effect on S_{11} levels, particularly in the upper band, while there is no significant effect observed when the gap between the outer and inner loops is varied in the range of 0.3–0.7 mm with noting that it is set to 0.5 mm in the final design.

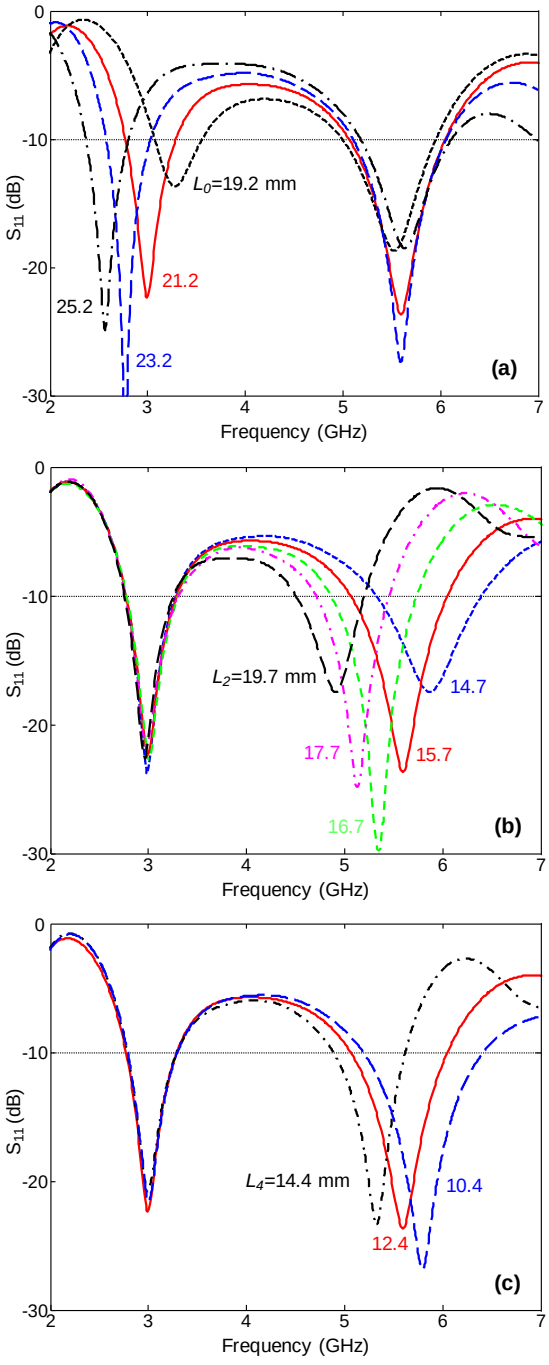

Fig. 9. The effects of (a) the dipole length ($2L_0$) and the loop dimensions (b) L_2 and (c) L_4 on the S_{11} performance.

When the dipole-loop gap is increased from the optimum value of 0.3 mm to 0.5 mm, there is a slight bandwidth reduction, and also about 0.2 GHz downward frequency shift observed. Moreover, the loop-widths have some slight effect on the performance. In particular, ±0.2 mm variation in the widths (W_1 & W_2) results in an upward or downward shift (at most 0.1 GHz) in the upper frequency-band. Similarly, the placement of the loops along the dipole-length (L_5) plays a role in fine-tuning of the upper center-frequency. Note that there has been no significant influence on the lower-band as the loop parameters are varied.

We also remark that there has been no degradation observed in the radiation properties of the antenna for the parametric studies considered. Furthermore, the proposed design tends to have a capability of broadband dipole performance (instead of dual-band). That is, with an appropriate parameter optimization, the gap between the lower and upper frequency bands may be closed, so the bands are joined together to provide a rather larger bandwidth performance. In Fig. 10, we display S_{11} characteristics of such a broadband design. As seen, this preliminary design offers 52.5% bandwidth (2.95–5.05 GHz) where $|S_{11}| < -6$ dB. We also note that the computed realized gain is 6–8 dB over the band of interest where radiation patterns are similar to those in Fig. 8.

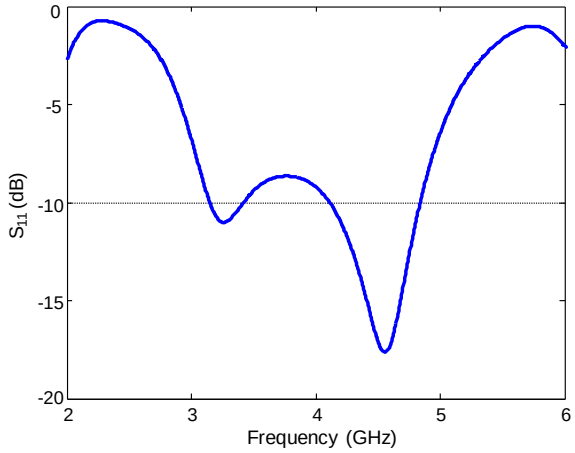

Fig. 10. The input reflection coefficient characteristics of the broadband LLPD/balun design where the parameters are same as those in Fig. 1 and Fig. 2 except W_0=2.9, L_0=19.1, L_2=18.75, L_3=13.55, L_5=7.3, l_3= 3 (all in mm).

Furthermore, an equivalent circuit modeling (ECM) for the LLPD design has been considered in this study. As seen in Fig. 11, the proposed simplistic model is based on the equivalent circuit models for the dipole antenna [20] and the loop elements [21]. By integrating those two models and including an additional capacitor (C_3) representing the coupling between the dipole and the loops, we obtained the ECM for the LLPD antenna. The corresponding capacitance, inductance, and resistance values (C_0=3.15 nF, L_0=0.2 nH, R_1=80 Ω, C_1=3 pF, L_1=0.7nH, R_2=2 Ω, C_2=1.4 pF, L_2=0.4 nH, R_3=11 Ω, C_3=0.9 pF) in the model were acquired by means of a curve-fitting algorithm considering only the related S_{11} magnitude for the design parameters given in Fig. 1. As shown in Fig. 12, the proposed ECM predicts the operational bands reasonably well with some differences in the out-of-bands. We note that in the ECM, R_1 mainly represents the radiation resistance of the dipole antenna, whereas the resistive elements R_2 and R_3 stand for possible physical losses. We note that those circuit element values will change if any dimension in the structure is altered. One can also develop empirical formulae relating the ECM values with the corresponding physical design parameters [1].

IV. CONCLUSION

In this paper, we have introduced a novel loop-loaded printed dipole antenna for a dual-band application operating at 3 GHz and 5.5 GHz bands. The proposed design has two new features: While the loop elements placed on the antenna aperture provides dual-band operation at the designated frequencies, the wideband balun/feed allows for matched and balanced excitation for the dipole. The practical realization of the proposed LLPD/balun design was carried out, resulting in reasonably good performance in accordance with the simulations. In particular, the design offers 15% impedance bandwidths at the corresponding bands with a fairly well radiation performance. We remark that the proposed low-profile antenna is simple in structure and can easily be adapted for different operational frequencies to be employed in various communications applications. Also, the proposed design can readily be extended to an array configuration. Finally, a simplistic equivalent circuit model for the LLPD antenna has

been proposed, predicting the antenna performance quite well.

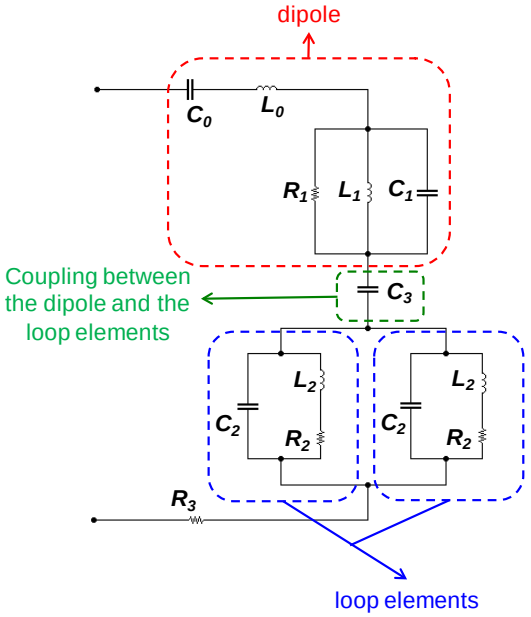

Fig. 11. The proposed equivalent circuit model for the LLPD antenna.

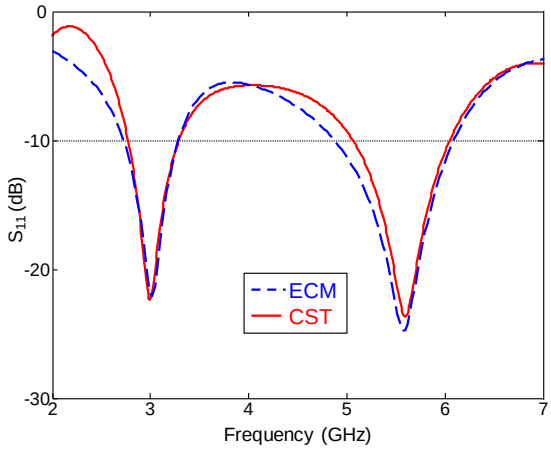

Fig. 12. The comparison of S_{11} characteristics for the simulated (CST) and the equivalent circuit model (ECM) of the LLPD antenna.

ACKNOWLEDGMENT

This work was supported by the Scientific & Technological Research Council of Turkey (TÜBİTAK–107E198) and partly funded by the Scientific Research Projects Unit of Kocaeli University (KOU–2010/35). We would like to thank all the reviewers for their invaluable comments.

REFERENCES

[1] Y. E. Erdemli, K. Sertel, R. A. Gilbert, D. E. Wright, and J. L. Volakis, "Frequency Selective Surfaces to Enhance Performance of Broadband Reconfigurable Arrays," *IEEE Trans. Antennas Propag.*, vol. 50, no. 12, pp. 1716-1724, 2002.

[2] A. Sondas, M. H. B. Ucar, and Y. E. Erdemli, "Tunable SRR-Based Substrate for a Microstrip Patch Antenna," *Turkish J. Elec. Eng. & Comp. Sci.*, vol. 20, no. 1, pp. 159-168, 2012.

[3] F. J. Herraiz-Martinez, L. E. Garcia-Munozle, D. Segovia-Vargas, D. Gonzalez-Overjero, and C. Craeye, "Arrays of Dual-Band Printed Dipoles Loaded with Metamaterial Particles," *3rd European Conf. Antennas and Propag. (EuCAP)*, pp. 3818-3822, Mar. 2009.

[4] J. -M. Floc'h and H. Rmili, "Design of Multiband Printed Dipole Antennas using Parasitic Elements," *Microwave Opt. Technol. Lett.*, vol. 48, no. 8, pp. 1639-1645, Aug. 2006.

[5] W. X. An, K. L. Lau, S. F. Li, and Q. Xue, "Wideband E-Shaped Dipole Antenna with Staircase-Shaped Feeding Strip," *Electronics Letters*, vol. 46, no. 24, pp. 1583-1584, 2010.

[6] H. Wong, K.-M. Mak, K.-M. Luk, "Wideband Shorted Bowtie Patch Antenna with Electric Dipole," *IEEE Trans. Antennas Propag.*, vol. 56, no. 7, pp. 2098-2101, 2008.

[7] Q. Wu, R. Jin, J. Geng, D. Su, "On the Performance of Printed Dipole Antenna with Novel Composite Corrugated-Reflectors for Low-Profile Ultrawideband Applications," *IEEE Trans. Antennas Propag.*, vol. 58, no. 12, pp. 3839-3846, 2010.

[8] X. N. Low, Z. N. Chen, W. K. Toh, "Ultrawideband Suspended Plate Antenna with Enhanced Impedance and Radiation Performance," *IEEE Trans. Antennas Propag.*, vol. 56, no. 8, pp. 2490-2495, 2008.

[9] W.-S. Chen and Y.-H. Yu, "Dual-Band Printed Dipole Antenna with Parasitic Element for WiMAX Applications," *Electronics Letters*, vol. 44, no. 23, pp. 1338-1339, 2008.

[10] V. Gonzalez-Posadas, J. L. Jimenez-Martin, F. J. Herraiz-Martinez, L. E. Garcia-Munoz, and D. Segovia-Vargas, "Design of Dual-Frequency SRR-Loaded Dipole with Equivalent Circuit Approach," *Electronics Letters*, vol. 45, no. 19, pp. 964-966, 2009.

[11] A. Sondas, M. H. B. Ucar, and Y. E. Erdemli, "Switchable Loop-Loaded Printed Dipole Antenna with a Balun/Feed Structure," *Microwave Optical Tech. Letts.*, vol. 54, no. 1, pp. 76-79, Jan. 2012.

[12] M. Naghshvarian-Jahromi and N. Komjani-Barchloui, "Analysis of the Behavior of Sierpinski Carpet Monopole Antenna," *Applied*

Computational Electromagnetics Society (*ACES*) *Journal*, vol. 24, no. 1, pp. 32-36, February 2009.

[13] J. C. Liu, W. Shao, and B. Z. Wang, "A Dual-Band Metamaterial Design using Double SRR Structures," *Applied Computational Electromagnetic Society (ACES) Journal*, vol. 26, no. 6, pp. 459-463, June 2011.

[14] R. Bakshi and S. K. Sharma, "A Wideband U-Slot Loaded Modified E-Shape Microstrip Patch Antenna and Frequency Agile Behavior by Employing Different Height Ground Plane and Ribbon Type Switches," *Applied Computational Electromagnetic Society (ACES) Journal*, vol. 26, no. 7, pp. 539-550, July 2011.

[15] Y. Zhao, L. Zhong, J. S. Hong, and G. M. Zhang, "A Monopole Antenna with SIR Ground for Harmonic Suppression and Bandwidth Enhancement," *Applied Computational Electromagnetic Society (ACES) Journal*, vol. 26, no. 8, pp. 705-708, August 2011.

[16] I. I. Papadopoulos-Kelidis, A. X. Lalas, N. V. Kantartzis, and T. D. Tsiboukis, "Combined Bowtie Peano Antennas for Wideband Performance," *Applied Computational Electromagnetic Society (ACES) Journal*, vol. 26, no. 9, pp. 760-767, Sep. 2011.

[17] A. Sondas, M. H. B. Ucar, and Y. E. Erdemli, "Dual-Band Loop-Loaded Printed Dipole Array," *Mediterranean Microwave Symposium (MMS)*, pp. 62-64, Guzelyurt, 25-27 Aug. 2010.

[18] A. Sondas, M. H. B. Ucar, and Y. E. Erdemli, "Tunable Loop-Loaded Printed Dipole Antenna Design," *IEEE Int. Symp. Antennas Propagat.*, Toronto, Canada, pp. 1-4, 11-17 July 2010.

[19] T. Xia, S. Yang, and Z. Nie, "Design of a Tapered Balun for Broadband Arrays with Closely Spaced Elements," *IEEE Antennas and Wireless Propagation Letters*, vol. 8, pp. 1291-1294, 2009.

[20] M. Hamid and R. Hamid, "Equivalent Circuit of Dipole Antenna of Arbitrary Length," *IEEE Trans. Antennas Propagat.*, vol. 45, no. 11, pp. 1695-1696, 1997.

[21] L. -H. Hsieh and K. Chang, "Equivalent Lumped Elements G, L, C, and Unloaded Q's of Closed- and Open-Loop Ring Resonators," *IEEE Trans. Microwave Theory Techniques*, vol. 50, no. 2, pp. 453-460, 2002.

Mustafa H. B. Ucar was born in Istanbul, Turkey, in 1982. He received the B.S. and M.S. degrees from the Kocaeli University, Kocaeli, Turkey both in Electronics & Computer Education Department in 2004 and 2007, respectively. He is currently a Ph.D. candidate and a research assistant in the same institution. His research interests include numerical analysis and design of reconfigurable antennas/arrays/EM filters and frequency selective surfaces.

Adnan Sondas was born in Tokat, Turkey, in 1978. He received the B.S. degree from the Sakarya University, Sakarya, in Electronics & Computer Education Department in 2001 and the M.S. and Ph.D. degrees from the Kocaeli University, Kocaeli, both in Electronics & Computer Education Department, in 2005 and 2011, respectively. He is currently a research assistant in Electronics and Computer Education at Kocaeli University. His research interests include numerical analysis and design of metamaterials, reconfigurable antennas/arrays/EM filters.

Yunus E. Erdemli was born in Tatvan, Turkey, in 1970. He received the B.S. degree in electrical engineering from Middle East Technical University, Ankara, Turkey, in 1992 and the M.S. and Ph.D. degrees from the University of Michigan, Ann Arbor, both in electrical engineering, in 1996 and 2002, respectively. During 1994–2002, he was a graduate Research Assistant at the University of Michigan Radiation Laboratory, Ann Arbor, where he also served as a Postdoctoral Research Associate. He has been a Professor in the Department of Electronics and Computer Education, Kocaeli University, Kocaeli, Turkey since 2002. His research interests include numerical analysis and design of conformal and reconfigurable arrays, frequency selective surfaces/volumes, and metamaterials for various communication applications.